

## Research paper

# Intra-laboratory assessment of a method for the detection of TiO<sub>2</sub> nanoparticles present in sunscreens based on multi-detector asymmetrical flow field-flow fractionation

Milica Velimirovic<sup>a,b</sup>, Stephan Wagner<sup>a,c</sup>, Robert Koeber<sup>d</sup>, Thilo Hofmann<sup>a</sup>, Frank von der Kammer<sup>a,\*</sup>

<sup>a</sup> Department of Environmental Geosciences, Centre for Microbiology and Environmental Systems Science, University of Vienna, Althanstrasse 14, 1090 Vienna, Austria

<sup>b</sup> Ghent University, Department of Chemistry, Atomic & Mass Spectrometry – A&MS research group, Campus Sterre, Krijgslaan 281-S12, 9000 Ghent, Belgium

<sup>c</sup> Helmholtz-Centre for Environmental Research - UFZ, Leipzig, Germany

<sup>d</sup> European Commission, Joint Research Centre, Geel, Belgium



## ARTICLE INFO

## Keywords:

TiO<sub>2</sub> nanoparticles in sunscreen  
Sample preparation  
Asymmetrical flow field-flow fractionation  
Multi angle light scattering  
ICP-MS  
In-house validation

## ABSTRACT

In this study, an intra-laboratory assessment was carried out to establish the effectiveness of a method for the detection of TiO<sub>2</sub> engineered nanoparticles (ENPs) present in sunscreen containing nano-scale TiO<sub>2</sub> and a higher nanometer-range (approx. 200–500 nm) TiO<sub>2</sub>, as well as iron oxide particles. Three replicate measurements were performed on five separate days to generate the measurement uncertainties associated with the quantitative asymmetrical flow field-flow fractionation (AF4) measurement of the hydrodynamic radius  $r_{h,mode1}$  (MALS),  $r_{h,mode1}$  (ICP-MS),  $r_{h,mode2}$  (ICP-MS), and calculated mass-based particle size distribution ( $d_{10}$ ,  $d_{50}$ ,  $d_{90}$ ). The validation study demonstrates that the analysis of TiO<sub>2</sub> ENPs present in sunscreen by AF4 separation-multi detection produces quantitative data (mass-based particle size distribution) after applying the sample preparation method developed within the NanoDefine project with uncertainties based on the precision ( $u_p$ ) of 3.9–8.8%. This method can, therefore, be considered as the method with a good precision. Finally, the bias data shows that the trueness of the method ( $u_t = 5.5$ –52%) can only be taken as a proxy due to the lack of a sunscreen standard containing certified TiO<sub>2</sub> ENPs.

## 1. Introduction

The current EU Cosmetic Products Regulation (EU Regulation (EC) No 1223/2009) requires the labeling of products containing engineered nanoparticles (ENPs) (EC, 2009). The characterization of ENPs has to be carried out not only with the pristine material, but also in the final cosmetic formulation (EC, 2016). Therefore, reliable and robust analytical methodologies that are fit-for-purpose and that have successfully made their way through a tedious and exhaustive validation process including intra- and interlaboratory comparisons are a prerequisite for the successful application of the Regulation itself. The major source of possible ENPs appearance in cosmetics are sunscreens with a high UVA and UVB protection factor (e.g., TiO<sub>2</sub> and ZnO ENPs), long-lasting make-ups (e.g., TiO<sub>2</sub> ENPs), anti-aging creams (e.g., TiO<sub>2</sub> and ZnO ENPs), lipsticks (e.g., TiO<sub>2</sub> ENPs), toothpastes (e.g., SiO<sub>2</sub>, TiO<sub>2</sub>, and Al<sub>2</sub>O<sub>3</sub> ENPs), and hair care or coloring products (e.g., TiO<sub>2</sub> and Fe<sub>2</sub>O<sub>3</sub> ENPs) (Contado and Pagnoni, 2008). TiO<sub>2</sub> ENPs appearing in

sunscreens are among the most studied ones in terms of the sample preparation method development and particle characterization (Contado and Pagnoni, 2008; Nischwitz and Goenaga-Infante, 2012; López-Heras et al., 2014; Müller et al., 2016; Philippe et al., 2018; Bocca et al., 2018; de la Calle et al., 2018). However, to our knowledge, most of the studies rely on time-consuming stepwise sample preparation procedures (Kammer et al., 2012) requiring the extraction of TiO<sub>2</sub> ENPs from sunscreen and further characterization in terms of particle size distribution by separation techniques such as field-flow fractionation (FFF) (Contado and Pagnoni, 2008; Nischwitz and Goenaga-Infante, 2012; López-Heras et al., 2014; Müller et al., 2016; Philippe et al., 2018; Bocca et al., 2018; de la Calle et al., 2018). Although promising, no thorough standardization and validation of the methods with respect to both sample preparation and multi-detector asymmetrical flow field-flow fractionation has been reported up to date (Babick et al., 2016; Gao and Lowry, 2018).

A quick and straightforward sample preparation method based on

\* Corresponding author.

E-mail address: [frank.kammer@univie.ac.at](mailto:frank.kammer@univie.ac.at) (F. von der Kammer).

<https://doi.org/10.1016/j.impact.2020.100233>

Received 22 April 2020; Received in revised form 17 June 2020; Accepted 19 June 2020

Available online 25 June 2020

2452-0748/ © 2020 The Authors. Published by Elsevier B.V. This is an open access article under the CC BY license (<http://creativecommons.org/licenses/by/4.0/>).

dilution by a cleaning agent and subsequent particle stabilization step to directly determine TiO<sub>2</sub> ENPs particle size distribution present in commercial sunscreen was recently reported (Velimirovic et al., 2020). Minimal alteration of the TiO<sub>2</sub> ENPs characteristics were demonstrated by a combination of asymmetrical flow field-flow fractionation (AF4) hyphenated to multi angle light scattering (MALS) and inductively coupled plasma–mass spectrometry (ICP-MS) (Velimirovic et al., 2020). The correctness of this analytical method was provided by internal particle size validation and comparison to a standard sample of TiO<sub>2</sub> ENPs of known size distribution in a realistic matrix following the generic sample preparation procedure proposed by Wagner et al. (Wagner et al., 2015). However, the reported analytical method still requires standardization in order to be applied in different laboratories. Therefore, the validation of the analytical method is necessary to achieve reproducibility, as well as reliability for routine use (Gao and Lowry, 2018).

This paper presents the results of an intra-laboratory assessment which examines the AF4-MALS-ICP-MS method for the characterization of TiO<sub>2</sub> ENPs. The method assesses the hydrodynamic radius  $r_{h,mode1}$  (MALS),  $r_{h,mode1}$  (ICP-MS),  $r_{h,mode2}$  (ICP-MS), and calculated mass-based particle size distribution (PSD,  $d_{10}$ ,  $d_{50}$ ,  $d_{90}$ ) present in the sunscreen consisting of nano-scale TiO<sub>2</sub> and submicroscale TiO<sub>2</sub> and iron oxide particles at the higher end of the nanometer size range (approx. 200–500 nm) after applying the straightforward sample preparation procedure developed within the NanoDefine project and adapting the AF4-MALS-ICP-MS conditions to some extent (Velimirovic et al., 2020). The validation of the sunscreen method was based on a generic approach for the validation of methods for the detection and quantification of nanoparticles in food samples previously reported by Linsinger et al. (Linsinger et al., 2013) determining the TiO<sub>2</sub> ENPs particle size distribution and chemical identity. Finally, the method parameters being working range, linearity and calibration, limit of detection (LOD)/limit of quantification (LOQ), selectivity, repeatability/intermediate precision, robustness, trueness, and measurement uncertainty were calculated following the recommendations set out by IUPAC in “Harmonized Guidelines for Single-Laboratory Validation of Analytical Methods” (Thompson et al., 2002), the Eurachem Guide “Fitness for Purpose of Analytical Methods” (Holcombe, 1998) and the Commission Decision 2002/657/EC on the reliability of methods for residues and contaminants in food of animal origin (EC, 2002).

## 2. Materials and methods

### 2.1. Chemicals

The Milli-Q water (MQ-water) used throughout the study was prepared using a PURELAB® Chorus 3 Ultrapure Water Purification System (ElgaLab Water, UK). Sodium chloride (analytical grade) and sodium dodecyl sulfate (SDS, Bio reagent, purity  $\geq 98.5\%$ ) were purchased from Sigma Aldrich. The commercial surfactant mixture Fisherbrand™ FL-70™ Concentrate was purchased from Fisher Scientific (USA, New Jersey). The cleaning agent (Denk mit Ultra) was purchased from DM, Germany. For testing the robustness of the method, dishwashing liquid (Pril) was purchased from Henkel, Austria. The pH values were measured with a Metrohm 6.0234.100 electrode (Metrohm, Switzerland). Different concentrations of NaOH solution (0.01, 0.1, and 1 mol/L NaOH) were prepared from NaOH pellets (Merck, analytical grade, USA) and MQ-water which were used for pH adjustment. Nanosphere™ latex beads of  $20 \pm 2$ ,  $46 \pm 2$ ,  $81 \pm 2.7$ ,  $102 \pm 3$ ,  $147 \pm 3$ ,  $199 \pm 6$  and  $269 \pm 5$  nm diameter were purchased from Duke Scientific (PaloAlto, CA, USA) for the calibration of the AF4 channel. The respective NIST traceable diameters as determined either by DLS or TEM are given in parenthesis. The TraceCERT® Ti reference standard of 1000 mg/L in 2–3% nitric acid was obtained from Merck (Darmstadt, Germany).

### 2.2. Samples

The complete formulation of sunscreen, containing nano-scale TiO<sub>2</sub> and a higher nanometer-range (approx. 200–500 nm) TiO<sub>2</sub> ( $55 \pm 1.5$  g TiO<sub>2</sub> /kg;  $N = 4$ ) and higher nanometer-range iron oxide ( $11 \pm 0.4$  g Fe<sub>2</sub>O<sub>3</sub> /kg;  $N = 4$ ) was selected as the representative test material within the NanoDefine project for its market relevance. The intra-laboratory assessment included the sample preparation procedure and the AF4-MALS-ICP-MS method. To assess the trueness of the method, a mixture of well-characterized TiO<sub>2</sub>-material (NM104, JRC, Institute for Reference Materials and Measurements) and a blank sunscreen formulation containing no TiO<sub>2</sub> ENPs or other inorganic particles were prepared to obtain a final concentration of 10 g TiO<sub>2</sub> /kg (SI1). A pure suspension of NM104 particles ( $c(\text{TiO}_2) = 1\%w/v$ ) was prepared according to the dispersion protocol provided in SI2 and was used as an in-house reference sample for assessing the bias of AF4-MALS-ICP-MS method.

### 2.3. Sample preparation procedure

The sunscreen sample was prepared by following the stepwise dilution of the sunscreen with a cleaning agent suitable to dissolve organic compounds typically present in sunscreen and particle stabilization step using the SDS (Velimirovic et al., 2020). Briefly, 10 mg of sunscreen sample was weighted in a 10 mL centrifuge glass vial and 1% (v/v) cleaning agent (Denk mit Ultra from DM) in MQ-water was added to give a sunscreen concentration of 1 mg/mL. The sample was shaken for 10 min horizontally until a homogeneous appearance was obtained and subsequently sonicated for 15 min in an ultrasonic water bath (Sonorex RK 106, Ø 240 mm, 130 mm high, 120 W effective power, BANDELIN Electronic GmbH & Co. KG, Germany). 2 mL of the sonicated sample were transferred to an empty glass vial and 2 mL of 0.2% SDS (m/v) solution were added (pH = 8.5–9) in order to avoid particle aggregation. The sample was sonicated for 5 min and left overnight. After ultrasonication for 15 min in an ultrasonic water bath, the sample was diluted 1:4 in 0.1% (v/v) SDS (prepared by diluting 0.2% SDS in MQ-water by a factor of 2 and filtered through Anodisc 0.02 µm nominal pore size membrane filters purchased from Whatman, Maidstone, UK) and sonicated for 2 min.

### 2.4. AF4-MALS-ICP-MS

The experimental conditions for the AF4 experiments and for the ICP-MS measurements are adapted from Velimirovic et al. (Velimirovic et al., 2020) and summarized in Table 1. The AF4 system used in this study consisted of an Agilent 1200 series auto sampler (G1329A), a quaternary high-performance liquid chromatography pump equipped with a micro vacuum degasser (G1311C) (Agilent Technologies, CA, USA), an Eclipse Dualtec flow control module, and a long AF<sup>4</sup> separation channel (Wyatt Technology, Dernbach, Germany) with a 350 µm spacer and regenerated cellulose membrane of 10 kDa (Millipore, Darmstadt, Germany). Due to the complexity of the samples the membranes were changed every second day performing approximately 15 runs on the same membrane. 0.025% (v/v) FL-70™ was used as a carrier solution and was filtered through an Anodisc 0.02 µm membrane filters (Whatman, Maidstone, UK) prior to use. The AF4 separation program used a detector flow of 1.0 mL/min and a constant cross flow rate of 0.6 mL/min. The AF4 system was coupled online with a MALS detector with 17 + 1 observation angles operated (15 usable in aqueous medium with online DLS attached to angle 11) and a linear polarized laser at 658 nm (DAWN® EOS™, Wyatt Technology Europe GmbH, Dernbach, Germany). The data acquisition interval was set to 2 s. Size calibration of the AF4 channel was performed under similar run conditions and the hydrodynamic radius ( $r_h$ ) was calculated using the calibration function determined in fractionations of the  $20 \pm 2$  nm (0.005% w/v),  $46 \pm 2$  nm (0.001% w/v),  $81 \pm 2.7$  nm (0.001% w/v),

**Table 1**

AF4 and ICP-MS operational parameters used for TiO<sub>2</sub> and Fe<sub>2</sub>O<sub>3</sub> ENPs characterization.

AF <sup>4</sup>	Unit	Value
Tip to tip channel length	[cm]	27.5
Spacer	[ $\mu$ m]	350
Focus flow rate	[ml/min]	0.60
Injection flow	[ml/min]	0.2
Injection time	[min]	8
Focus time	[min]	2
Elution time	[min]	50
Detector flow rate	[mL/min]	1
Cross flow rate	[mL/min]	0.6
Membrane		Regenerated cellulose (RC), 10 kDa, Millipore
Carrier		0.025% (v/v) FL-70™
Injection volume	[ $\mu$ L]	100
ICP-MS		
RF power	[W]	1600
Sample depth	[mm]	10
Gas flow rates		
-Carrier gas	[L/min]	1.06
-Make up gas	[L/min]	0.35
- He	[mL/min]	4.5
- O <sub>2</sub>	[mL/min]	0.4
Sample uptake rate	[mL/min]	0.3 (established by split flow)
Nebulizer		MICROMIST (Glass Expansion)
Spray chamber		Scott double-pass
Isotopes monitored		<sup>47</sup> Ti and <sup>56</sup> Fe
Integration time per isotope	[ms]	1500

Size calibrations of the AF4 channel were performed under similar run conditions.

102 ± 3 nm (0.0005% w/v), 147 ± 3 nm (0.0005% w/v), 199 ± 6 nm (0.0001% w/v) and 269 ± 5 nm (0.0001% w/v) diameter Nanosphere™ standards after subtracting the time of the void peak (the peak from unretained compounds). An online coupled ICP-MS (Agilent 8800, Agilent Technologies, USA) has been used to measure isotopes <sup>47</sup>Ti and <sup>56</sup>Fe considering that the main spectroscopic interferences on these masses were removed. The ICP-MS measurements were calibrated using dissolved Ti. The mass concentration of the Ti has been converted to TiO<sub>2</sub> mass eluting from the AF4. A background solution of 0.025% (v/v) FL-70™ was used during calibration of the ICP-MS to take into account any possible interferences and matrix effects arising from the constituents of FL-70™ in the AF4 carrier. The concentration of the calibration standards included 0; 1.25; 2.5; 5; 10; 25; and 50  $\mu$ g Ti /L. Calibration functions for converting the ICP-MS signals to concentrations were set up by plotting the averaged intensities of standard solutions against the standard concentrations, after subtracting the background signal. The signal intensities in the fractograms were then converted into concentration values. These data were further processed in Origin9.1 by substitution of every 8 data with an average value. Finally, advanced baseline processing was done in PeakFit™ v4.12 using 2nd Deriv Zero algorithm with quadratic option (PeakFit™ v4 Users Guide, SeaSolve Software Inc., 2003).

## 2.5. Experimental set up

A nested design experimental setup was applied (Linsinger et al., 2013; Thompson et al., 2002; Magnusson and Örnemark, 2014) in order to evaluate repeatability and intermediate precision of the method. Measurements were spread over 5 days with 3 replicate analyses per day by a single test person that performed all the experiments (Fig. 1).

## 2.6. Uncertainty calculations

The repeatability variance ( $s_r$ ), between-day variance ( $s_{day}$ ), and the time-different intermediate precision ( $s_{IP}$ ) of  $r_{h,model1}$  (MALS),  $r_{h,model1}$

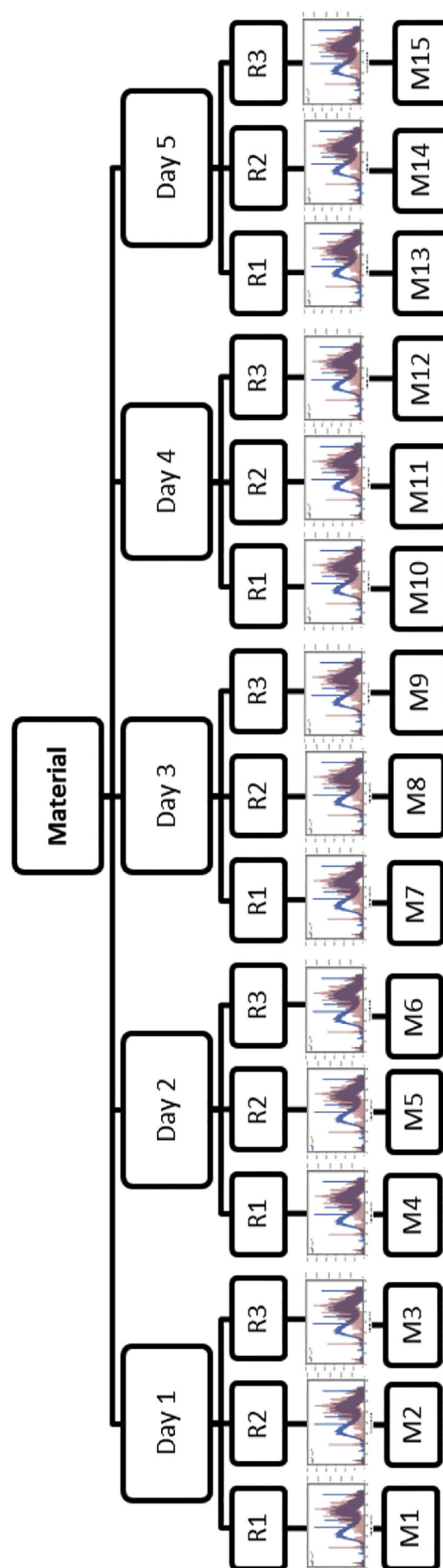


Fig. 1. A schematic representation of the experimental design of the intra-laboratory validation study. R = repetition and M = measurement.

(ICP-MS),  $r_{h,mode2}$  (ICP-MS), and mass-based PSD ( $d_{10}$ ,  $d_{50}$ ,  $d_{90}$ ) and the respective uncertainties associated to repeatability ( $u_r$ ), to day-to-day variation ( $u_{day}$ ), and to intermediate precision ( $u_{IP}$ ) were calculated from the nested design experiments (3 repeats on 5 separate days). The approach followed IUPAC and Eurachem guidelines (Thompson et al., 2002; Holcombe, 1998) and the European Commission Decision on the reliability of methods for residues and contaminants in food of animal origin (2002/657/EC) (EC, 2002). The combined measurement uncertainty ( $u_c$ ) included contributions due to repeatability ( $u_r$ ), day-to-day variations ( $u_{day}$ ), and trueness ( $u_t$ ). In order to calculate  $u_t$ , the uncertainty due to bias ( $u_b$ ) was calculated. Finally, the expanded measurement uncertainty  $U$  ( $k = 2$ ) was calculated. Details of the calculations are described in SI3.

### 3. Results and discussion

#### 3.1. Calibration, linearity and working range

##### 3.1.1. TiO<sub>2</sub> ENPs size

The particle size range of AF4 method is typically from 1 nm up to 1  $\mu$ m (de la Calle et al., 2018; Kammer et al., 2011). The working range of the applied AF4 method is defined by the lower and upper size limits of analyzed polystyrene reference materials as up to date different TiO<sub>2</sub> particle size reference materials are not available. The size calibration of the AF4 channel with the reference material other than the sample is acceptable as already addressed extensively in the literature (Wagner et al., 2015; Neubauer et al., 2013; Loeschner et al., 2015), as long as the ideal elution behavior for standards and the sample is achieved. A size-retention time calibration curve was established based on the analysis of 7 calibration materials (polystyrene reference materials) with assigned diameters ranging from (20  $\pm$  2) nm to (269  $\pm$  5) nm. The calibration curves were established by plotting the retention times ( $t_r$ ) for 90° MALS signal (i.e. modal values of the largest peak in fractograms) against the assigned diameters ( $d_h$ ) on three different days (SI4). The linear least squares fitting model was used to mathematically determine the degree of correlation between  $t_r$  and  $d_h$  and to provide linear regression. The slope coefficients of the calibration curve were 0.1482 (series 1), 0.1539 (series 2), and 0.1425 (series 3). The correlation coefficient ( $r$ ) of the linear fits of polystyrene reference materials calibration curves were 0.9997 (series 1), 0.9991 (series 2), and 0.9997 (series 3). The coefficient of determination ( $R^2$ ) was 0.9990 (series 1), 0.9971 (series 2), and 0.9995 (series 3). The regression analysis of the calibration curves for the polystyrene reference materials showed a linear relationship between  $t_r$  and  $d_h$  (the  $r$  value obtained after calibration must be equal or higher than 0.990).

##### 3.1.2. TiO<sub>2</sub> ENPs mass concentration

The use of the conventional Ti standard for the quantification of TiO<sub>2</sub> ENPs by AF4-ICP-MS was reported previously (Nischwitz and Goenaga-Infante, 2012; López-Heras et al., 2014). Therefore, the ICP-MS measurements were calibrated using matrix matched dissolved Ti standards. The off-line matrix matched Ti calibration was established using Ti solutions of different concentrations on five different days before AF4-MALS-ICP-MS analysis. A Ti mass calibration curve was established based on the analysis of 6 calibration points from 1.25  $\mu$ g/L to 50  $\mu$ g/L of dissolved Ti using the method of least squares (SI5) representing the working range in terms of Ti concentration of the method. The calibration curves (the ICP-MS <sup>47</sup>Ti signal intensity vs. Ti concentration in  $\mu$ g/L) were linear with  $r$  and  $R^2$  values  $\geq$  0.9990. The slope coefficients of the calibration curve were 111.30 (series 1), 109.92 (series 2), 132.99 (series 3), 133.31 (series 4), and 136.07 (series 5). The difference between slope coefficient for series 1 and 2 compared to series 3–5 can be explained by possible minor clogging of the nebulizer pointing out that the fresh calibration has to be prepared every day before AF4-MALS-ICP-MS analysis if internal standard is not used for checking the sensitivity of the detection system.

#### 3.2. Limit of detection (LOD)/Limit of quantification (LOQ)

##### 3.2.1. TiO<sub>2</sub> ENPs size

The commonly applied concepts of LOD/LOQ including the sigma criteria do not apply for size determination by AF4. In AF4, the smallest detectable particle size is equal to the smallest particle size used in the external calibration which was 20 nm in this study. The upper limit of quantification (ULOQ) is the largest particle size calibration standard on the calibration curve (269  $\pm$  5) nm, as the analyte response was reproducible.

##### 3.2.2. TiO<sub>2</sub> ENPs mass concentration

Three approaches were applied to determine the LOD and LOQ for the TiO<sub>2</sub> ENPs mass fraction. In the first approach the lower LOD and LOQ of the ICP-MS method for the quantification of dissolved Ti were estimated as 3.3 times and 10 times the standard deviation of the y-intercept taken from five calibration curves. The calculated LOD and LOQ were 2.1  $\pm$  0.3  $\mu$ g/L and 6.4  $\pm$  0.3  $\mu$ g/L, respectively.

Five independent subsamples of a blank sunscreen matrix containing no TiO<sub>2</sub>/Fe<sub>2</sub>O<sub>3</sub> particles subjected to the same stepwise dilution as the complete formulation of the sunscreen (Velimirovic et al., 2020) and analysis by ICP-MS has been selected as a second approach for the determination of the LOD and LOQ. The standard deviation of the dissolved Ti results was calculated and the lower LOD and LOQ were 1.3  $\pm$  0.1  $\mu$ g/L and 4.2  $\pm$  0.1  $\mu$ g/L, respectively. These results are 1.5–1.6 times lower than the LOD and LOQ values determined from the calibration curve approach.

A limit of detection for the entire analytical procedure (sample preparation followed by AF4-ICP-MS analysis) is determined from the standard deviation calculated from triplicate results obtained on three independent blank subsamples (sunscreen matrix containing no TiO<sub>2</sub>/Fe<sub>2</sub>O<sub>3</sub> particles) representing a complete and independent application of the method, including sample preparation steps (SI6) as previously proposed by Linsinger et al. (Linsinger et al., 2013). The lower LOD and LOQ for the quantification were 0.4  $\pm$  0.2  $\mu$ g/L and 1.3  $\pm$  0.8  $\mu$ g/L, respectively. The reported values of the third approach were significantly lower than those for the first and second approach, but with the higher uncertainty, and are the best representation of the expected LOD/LOQ for whole sample preparation procedure followed by AF4-MALS-ICP-MS analysis. The decreased LOD/LOQ values could be attributed to the sample dilution during AF4 separation which results in a decreased mass flux into the ICP-MS compared to analysis of dissolved constituents.

#### 3.3. Selectivity

In the case of consumer products, Linsinger et al. (Linsinger et al., 2013) proposed three scenarios that need to be addressed in order to assess method selectivity: (1) the selectivity against matrix constituents, (2) the selectivity against other types of ENPs, and (3) the presence of the same ENPs, but in a different form (e.g., size).

##### 3.3.1. Selectivity against matrix constituents

The selectivity of the AF4-MALS method towards TiO<sub>2</sub> ENPs against matrix constituents was evaluated by analyzing the blank sunscreen formulation containing no or other inorganic particles and comparison with the AF4-MALS data obtained for the complete formulation of sunscreen as suggested by others (Linsinger et al., 2013). In addition, AF4-MALS data obtained for the blank sunscreen formulation were compared with AF4-MALS data obtained for MQ-water (SI6) in order to exclude any particulate matter that was already present in the carrier solution. Comparing the fractograms of the blank sunscreen formulation and the complete formulation (Fig. 2a), it can be concluded that the AF4-MALS method can suffer from possible interference of the organic matrix (the blank sunscreen eluting at  $t_r = 20$ –40 min) and that the selectivity to distinguish between ENPs signal and sunscreen matrix



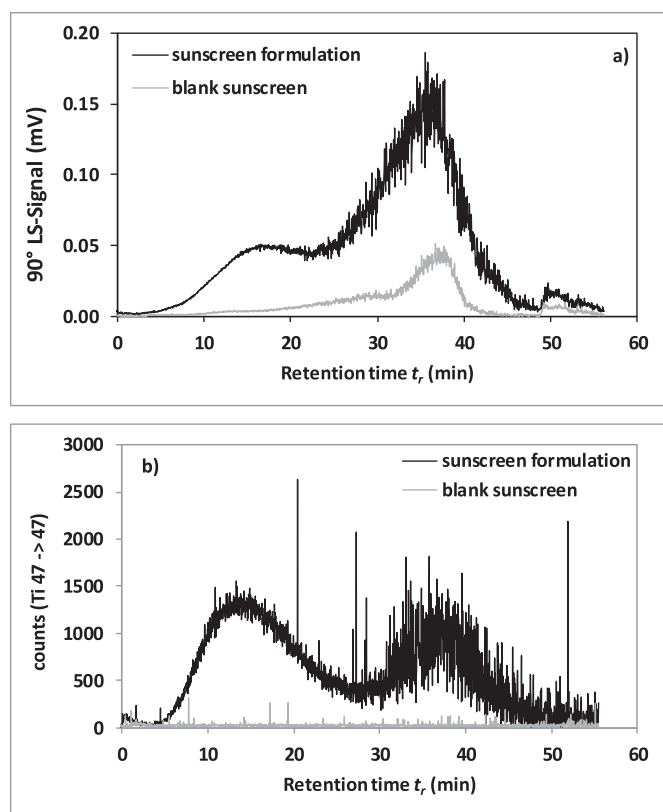


Fig. 2. Signal comparison for blank sunscreen sample (grey) and complete sunscreen formulation (black); a) light scattering signal ( $90^\circ$ ) and b) ICP-MS signal ( $^{47}\text{Ti}$ ). AF4-MALS fractogram obtained from injecting only the carrier solution is presented in SI6.

can be stated only for the first part of the complete formulation fractogram ( $t_r = 0\text{--}24$  min) where  $\text{TiO}_2$  ENPs are expected.

It was necessary to monitor the  $^{47}\text{Ti}$  signal for both the complete sunscreen formulation and the blank sunscreen by ICP-MS because the AF4-MALS method is not specific enough to distinguish particles based on their chemical composition, and because of the presence of the same particles in a different size (Fig. 2b). The comparison of AF4-ICP-MS fractograms for the blank sunscreen formulation and complete formulation of sunscreen shows that there are no indications that the blank sample contains  $\text{TiO}_2$  ENPs (Fig. 2b) or  $\text{Fe}_2\text{O}_3$  ENPs (SI7).

### 3.3.2. Selectivity against other types of ENPs

The AF4-MALS fractogram of the complete sunscreen formulation revealed the presence of a second particle population in the samples ( $t_r = 24\text{--}49$  min) that can be attributed to both  $\text{TiO}_2$  and  $\text{Fe}_2\text{O}_3$  particles present in the sample. However, the AF4-MALS provides only the size selectivity without chemical composition. The selectivity of the AF4 method to distinguish between the particles of different chemical compositions is assessed by monitoring of the  $^{56}\text{Fe}$  signal in parallel to the  $^{47}\text{Ti}$  signal (Fig. 3). The  $^{56}\text{Fe}$  signal indicates a particle population with  $r_h$  values larger than 100 nm with  $t_r = 20\text{--}50$  min. In the present case, selectivity against  $\text{Fe}_2\text{O}_3$  is possible.

### 3.3.3. Selectivity against same particles but in a different size

The presence of particles with the same chemical identity but in a different size was assessed by monitoring the  $^{47}\text{Ti}$  signal for the sunscreen formulation (Fig. 3) and comparing with EM results previously reported by Velimirovic et al. (Velimirovic et al., 2020). The ICP-MS data for  $^{47}\text{Ti}$  measurement showed a double peak fractogram. The second peak might be caused by larger particles or by aggregates/agglomerates of smaller  $\text{TiO}_2$  particles which is in accordance with the

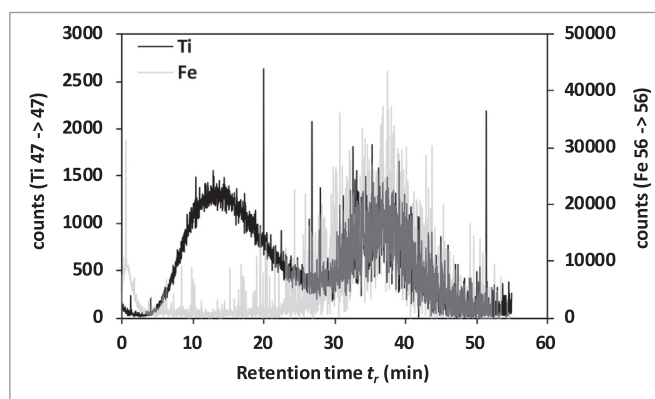


Fig. 3. The complete sunscreen formulation AF4-ICP-MS signal comparison ( $^{47}\text{Ti}$ ) and ( $^{56}\text{Fe}$ ).

reported EM data (Velimirovic et al., 2020).

### 3.3.4. Repeatability/intermediate precision

The evaluation of repeatability and the calculation of intermediate precision was assessed by nested design experimental set up measuring triplicate samples over 5 different days. The measured parameters of the  $\text{TiO}_2$  particle size distribution (Fig. 4a) present in the sunscreen were:  $r_{h,\text{mode1}}$  (ICP-MS),  $r_{h,\text{mode2}}$  (ICP-MS), and mass-based PSD ( $d_{10}$ ,  $d_{50}$ ,  $d_{90}$ ).  $r_{h,\text{mode1}}$  (MALS) is considered as  $\text{TiO}_2$  specific, while  $r_{h,\text{mode2}}$  (MALS) is not included as the second peak of AF4-MALS fractogram might be influenced by organic matrix of sunscreen as well as  $\text{TiO}_2/\text{Fe}_2\text{O}_3$  microscale-particles (Fig. 4b).

The  $r_{h,\text{mode1}}$  (MALS),  $r_{h,\text{mode1}}$  (ICP-MS),  $r_{h,\text{mode2}}$  (ICP-MS) for 15 runs

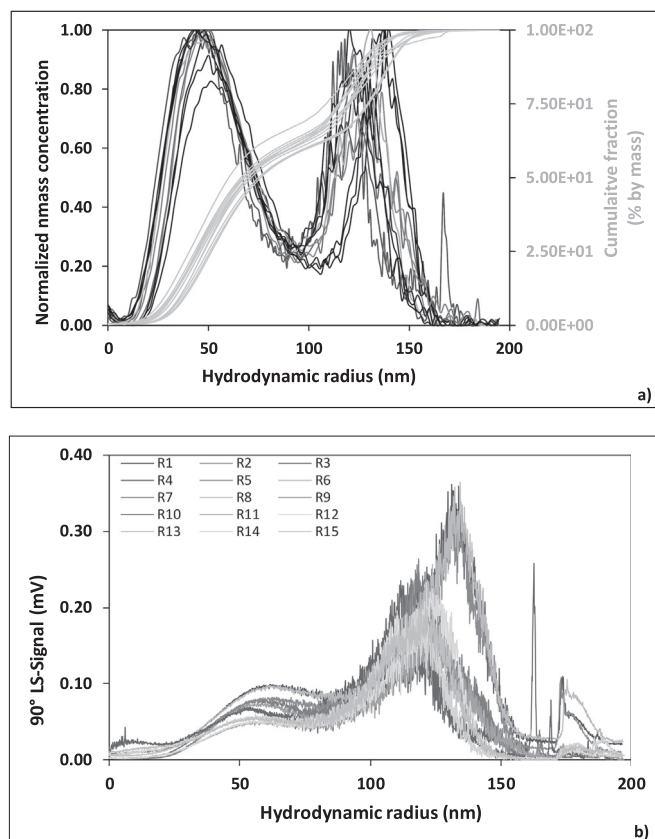


Fig. 4. (a) Mass-based  $\text{TiO}_2$  particle size distribution in the complete sunscreen formulation (R1-R15, black) and respective cumulative fraction (R1-R15, grey). (b) AF4-MALS fractograms of the complete sunscreen formulation.

**Table 2**

The repeatability variance ( $s_r$ ), between-day variance ( $s_{day}$ ), the time-different intermediate precision ( $s_{IP}$ ) and uncertainty values of  $r_{h,mode1}$  (MALS),  $r_{h,mode1}$  (ICP-MS),  $r_{h,mode2}$  (ICP-MS), and mass-based PSD ( $d_{10}$ ,  $d_{50}$ ,  $d_{90}$ ).

Size descriptor	MALS			ICP-MS			mass-based PSD		
	$r_{h,mode1}$			$r_{h,mode1}$			$r_{h,mode2}$		
	$d_{10}$	$d_{50}$	$d_{90}$	$d_{10}$	$d_{50}$	$d_{90}$	$d_{10}$	$d_{50}$	$d_{90}$
Number of replicates	15	15	15	15	15	15	15	15	15
Mean (nm)	<b>55</b>	<b>45</b>	<b>127</b>	<b>70</b>	<b>143</b>	<b>268</b>	<b>70</b>	<b>143</b>	<b>268</b>
sd	2.1	1.9	6.6	5.8	10	13	5.8	10	13
Min (nm)	52	43	117	62	127	251	62	127	251
Max (nm)	59	50	138	80	159	287	80	159	287
$s_r$	1.5	1.4	4.2	3.5	7.9	10.2	3.5	7.9	10.2
$s_{day}$	1.5	1.4	5.5	5.0	7.2	9.1	5.0	7.2	9.1
$s_{IP}$	2.1	2.0	6.9	6.1	10.6	13.6	6.1	10.6	13.6
$u_r$ (%)	2.7	3.2	3.3	5.1	5.5	3.8	5.1	5.5	3.8
$u_{day}$ (%)	2.8	3.1	4.4	7.1	5.0	3.4	7.1	5.0	3.4
$u_{IP}$ (%)	3.9	4.4	5.8	8.8	7.4	5.1	8.8	7.4	5.1

Variance of repeatability ( $s_r$ ), between-day variance ( $s_{day}$ ), and the time-different intermediate precision ( $s_{IP}$ ), uncertainty associated to repeatability ( $u_r$ ), uncertainty due to day-to-day variation ( $u_{day}$ ), and uncertainty associated to intermediate precision ( $u_{IP}$ ). Mean values of  $r_{h,mode1}$  (MALS),  $r_{h,mode1}$  (ICP-MS),  $r_{h,mode2}$  (ICP-MS), and mass-based PSD ( $d_{10}$ ,  $d_{50}$ ,  $d_{90}$ ) are presented in bold.

of sunscreen sample resulted in  $(55 \pm 2)$  nm,  $(45 \pm 2)$  nm, and  $(127 \pm 1)$  nm, respectively (Table 2). The results show that  $r_{h,mode1}$  (MALS),  $r_{h,mode1}$  (ICP-MS),  $r_{h,mode2}$  (ICP-MS), and the 10% and 50% of the mass-based PSD ( $d_{10}$ ,  $d_{50}$ ) were not significantly different ( $p < .05$ ). A slight difference was observed for the  $d_{90}$  ( $p = .054$ ). This was, however, expected because the largest particle size standard used for linear size calibration of the AF4 channel is  $269 \pm 5$  nm and retention times ( $t_r$ ) associated to the elution of larger particles might deviate from the linear fit due to the steric inversion effects (Velimirovic et al., 2020). Moreover, the observed deviations in the ICP-MS fractogram towards the larger particle size ( $r_h > 50$  nm or  $d_h > 100$  nm) can also affect the precision of the method as the larger particle size in the sample will occur in lower mass concentration compared to the smaller particle size. For explaining the significantly higher  $r_{h,mode1}$  (MALS) over the  $r_{h,mode1}$  (ICP-MS) the MALS signal that is intensity weighted and the ICP-MS signal that is mass weighted have to be taken into count. More in detail, scattering intensity increases with particle size which results in a shift of the MALS based size distribution towards larger particles compared to the ICP-MS based particle size distribution. In case a smaller MALS angle would be selected the signal would increase for larger particles as a consequence of smaller angles that have higher sensitivity for larger particles.

Determined uncertainties associated to repeatability ( $u_r$ ) and due to day-to-day variation ( $u_{day}$ ) for all size descriptors being  $r_{h,mode1}$  (MALS),  $r_{h,mode1}$  (ICP-MS),  $r_{h,mode2}$  (ICP-MS), and mass-based PSD ( $d_{10}$ ,  $d_{50}$ ,  $d_{90}$ ) were lower than 7.1%. This is realistic taking into account the complexity of the sunscreen sample, as well as the simplified sample preparation procedure followed by multi-detector AF4 analysis. The lowest  $u_r$  (2.7%) and  $u_{day}$  (2.8%) values were determined for  $r_{h,mode1}$  (MALS), indicating that AF4-MALS could successfully determine the particle size of the ENPs present in the sample. A similar outcome was observed for the AF4-ICP-MS data that could successfully detect and quantify the TiO<sub>2</sub> ENPs. Slightly higher  $u_r$  and  $u_{day}$  values determined for 10% and 50% of the mass-based PSD ( $d_{10}$ ,  $d_{50}$ ) indicate that the higher mass of the smaller particles in the sample contributes stronger to the uncertainty of the method. It has to be noted that  $u_{day}$  values for  $r_{h,mode1}$  (ICP-MS) and mass-based PSD ( $d_{50}$ ,  $d_{90}$ ) were lower than  $u_r$ . These low  $u_{day}$  values are achieved despite the changing of the AF4 membrane and consequently a new size calibrations every second day. Finally, the calculated uncertainty associated to intermediate precision ( $u_{IP}$ ) of 3.9% (for  $r_{h,mode1}$  (MALS)) to 8.8% (for  $d_{10}$ ) indicates that the

method for detection of TiO<sub>2</sub> ENPs present in sunscreen based on the AF4 separation-multidetector analysis is a method with a good precision (Table 2).

### 3.4. Robustness

Small but unavoidable variations during the sample preparation and the subsequent analysis can have a significant effect on the method performance and consequently the final particle size. The robustness of the method was tested by using a dishwashing liquid Pril (containing similar ingredients as cleaning agent) during the sample preparation procedure. The average value of mass-based TiO<sub>2</sub> PSD ( $d_{10}$ ,  $d_{50}$ ,  $d_{90}$ ) for the 3 replicate analyses that were performed in one day using the second cleaning agent is compared to the average value of the 15 replicate analysis that were performed over 5 days (S18) in order to access the robustness. By applying a different cleaning agent during the first step of the sample preparation procedure, the average value of mass-based TiO<sub>2</sub> PSD ( $d_{10}$ ,  $d_{50}$ ,  $d_{90}$ ) resulted in  $(55 \pm 1)$  nm,  $(96 \pm 2)$  nm, and  $(232 \pm 3)$  nm, respectively. The average difference between the mass-based TiO<sub>2</sub> PSD after introducing the different cleaning agent in the sample preparation method compared to the initial (Table 2) was  $23\% \pm 10\%$  underlying that the consistent use of the proposed cleaning agent is crucial for obtaining good data between different laboratories. Therefore, the consistent use of the cleaning agent is crucial for this method.

### 3.5. Approaches to evaluate trueness and recovery rate

#### 3.5.1. TiO<sub>2</sub> ENPs size

A certified reference material that consists of sunscreen with TiO<sub>2</sub> ENPs with a certified size or size distribution is not available. Therefore, the trueness of the determined size values was assessed by comparing the  $r_{h,mode}$  (MALS),  $r_{h,mode}$  (ICP-MS), and mass-based PSD ( $d_{10}$ ,  $d_{50}$ ,  $d_{90}$ ) of a suspension of NM104 particles ( $c(\text{TiO}_2) = 1\%$  w/v) and with a blank sunscreen matrix containing 10 g TiO<sub>2</sub> /kg of spiked NM104 (confirmed by the total digestion of the sample and further analysis by ICP-MS). The  $r_{h,mode}$  (MALS), and  $r_{h,mode}$  (ICP-MS) derived from AF4-MALS-ICP-MS analysis for the suspension of NM104 particles were  $(56 \pm 2)$  nm and  $(42 \pm 1)$  nm, respectively. Mass-based PSD ( $d_{10}$ ,  $d_{50}$ ,  $d_{90}$ ) were 57 nm, 97 nm, and 175 nm, respectively. These values are considered as reference values. Three replicates of spiked NM104 blank sunscreen samples (in-house reference sample) were measured in one day (each replicate represents the complete and independent sample preparation procedure). The  $r_{h,mode}$  (MALS) and  $r_{h,mode}$  (ICP-MS) were determined as  $(68 \pm 3)$  nm and  $(50 \pm 2)$  nm, respectively. Mass-based PSD ( $d_{10}$ ,  $d_{50}$ ,  $d_{90}$ ) of spiked NM104 blank sunscreen samples were 52 nm, 132 nm, and 227 nm, respectively. Comparing the reference values with the values measured for the blank sunscreen matrix spiked with NM104 (Table 3) a shift of the size distribution towards larger sizes was visible. Therefore, the calculated bias is higher than the expanded uncertainty of the bias (Table 3) indicating that there is a possible statistically significant trueness bias of the method.

The expanded uncertainty for  $r_{h,mode1}$  (MALS),  $r_{h,mode1}$  (ICP-MS), and  $r_{h,mode2}$  (ICP-MS) in the provided sunscreen sample was 25.3%, 17.1%, and 18.7%, respectively, taking into account uncertainty due to bias coming from spiking experiments (Table 4). These data show that even without certified reference material at satisfactory level of method precision can be reached. The largest effects calculated for  $d_{50}$  (71.5%) and  $d_{90}$  (104.5%) of mass-based PSD can be explained by the higher expected uncertainty towards the larger particle size. This data should be taken only as a proxy for trueness as the TiO<sub>2</sub> ENPs size data for NM104 dispersion and a blank sunscreen formulation which contains NM104 cannot be directly compared due to the possible agglomeration of NM104 with the constituents of the sunscreen during the spiking procedure. The change in the particle size and particle size distribution due to the sample preparation procedure has previously been pointed

**Table 3**

Summary table of the  $r_{h,mode}$  (MALS),  $r_{h,mode}$  (ICP-MS), and mass-based PSD ( $d_{10}$ ,  $d_{50}$ ,  $d_{90}$ ) for NM104 dispersion and the blank sunscreen matrix spiked with NM104 (presented in bold) and its contribution to the uncertainty associated with the bias.

	MALS	ICP-MS	Mass-based PSD		
	$r_{h,mode}$	$r_{h,mode}$	$d_{10}$	$d_{50}$	$d_{90}$
NM104 dispersion (nm)	<b>56</b>	<b>42</b>	<b>57</b>	<b>97</b>	<b>175</b>
sd	1.8	0.6	0.5	0.5	0.5
Blank + NM104 (nm)	<b>68</b>	<b>50</b>	<b>52</b>	<b>132</b>	<b>227</b>
sd	3.0	1.5	0.9	1.0	1.0
Bias =  C2 - C1	12.0	7.3	5.5	35.0	52.0
$u_b$ (%)	2.0	0.9	0.6	0.7	0.7
$U_b$ (%)	4.0	1.8	1.2	1.4	1.4
$u_c$ (%)	12.0	7.3	5.5	35.0	52.0

Uncertainty due to bias ( $u_b$ ), expanded uncertainty of the bias ( $U_b$ ), and uncertainty associated with trueness ( $u_t$ ).

**Table 4**

The combined and expanded measurement uncertainties for  $r_{h,mode}$  (MALS),  $r_{h,mode1}$  (ICP-MS),  $r_{h,mode2}$  (ICP-MS), and mass-based PSD ( $d_{10}$ ,  $d_{50}$ ,  $d_{90}$ ).

	MALS	ICP-MS		Mass-based PSD		
	$r_{h,mode}$	$r_{h,mode1}$	$r_{h,mode2}$	$d_{10}$	$d_{50}$	$d_{90}$
$u_c$ (%)	12.7	8.6	9.4	10.4	35.8	52.2
$U$ (%)	25.3	17.1	18.7	20.8	71.5	104.5

Combined uncertainty ( $u_c$ ), Expanded uncertainty ( $k = 2$ ):  $U$  (%).

out as an important issue that has to be taken into account during evaluating trueness of the FFF methods (Linsinger et al., 2013; Loeschner et al., 2015).

### 3.5.2. TiO<sub>2</sub> ENPs mass recovery

The performance of the sample preparation method and consequently AF4 performance was evaluated by the calculation of bulk Ti mass recovery ( $rec_{Ti,bulk}$ ) of the nominal Ti concentration in the sunscreen (54 g TiO<sub>2</sub>/kg determined in the total digested sunscreen sample and analyzed by ICP-MS following the previously reported digestion procedure)<sup>13</sup>. The blank sunscreen matrix spiked with NM104 after sample preparation procedure, as well as the AF4 recovery which was derived from the MALS signal ( $rec_{AF4-MALS}$ ) and the ICP-MS signal ( $rec_{AF4-ICP-MS}$ ). Total mass recoveries of  $\geq 80\%$  including the sample preparation and AF4 recoveries of  $\geq 80\%$  should be achieved as previously proposed by Wagner et al. (Wagner et al., 2015) in generic multi-step procedure for the development of a sample preparation method to extract ENPs from a complex matrix.

High average Ti bulk mass recovery rates ( $rec_{Ti,bulk} = 91\% \pm 14\%$ ; 5 days of 3 measurements each, total mean and standard deviation) were determined showing the high performance of the sample preparation procedure with no significant variance between the single samples (ANOVA,  $p < .05$ ). Recoveries determined using MALS detector ( $rec_{AF4-MALS}$ ) were  $84\% \pm 5\%$  (5 days of 3 measurements each, total mean and standard deviation). Recovery calculations based on <sup>47</sup>Ti ICP-MS signal ( $rec_{AF4-ICP-MS}$ ) were  $104\% \pm 5\%$  (5 days of 3 measurements each, total mean and standard deviation). The  $rec_{AF4-MALS}$  and  $rec_{AF4-ICP-MS}$  data indicate that there was little or no loss of particles during the fractionation process and that this method shows good performance.

As a proxy of trueness, the recovery of mass concentration of the blank sunscreen matrix spiked with NM104 was also determined as proposed by Linsinger et al. (Linsinger et al., 2013). Based on the Ti mass concentration for 3 replicates measured in one day (each replicate represents the complete and independent sample preparation procedure) the Ti bulk mass recovery ( $rec_{Ti,bulk}$ ) was  $75\% \pm 7\%$ . Recoveries

determined using MALS detector ( $rec_{AF4-MALS}$ ) and <sup>47</sup>Ti ICP-MS signal ( $rec_{AF4-ICP-MS}$ ) were  $107\% \pm 14\%$  and  $100\% \pm 14\%$ , respectively.

## 4. Conclusions

For the first time an intra-laboratory assessment of a sample preparation method followed by AF4-MALS-ICP-MS analysis for the detection and quantification of TiO<sub>2</sub> ENPs present in sunscreen has been carried out. The reported method gives the information on the TiO<sub>2</sub> ENPs particle size, chemical identity and mass-based PSD in order to fulfill the requirements of the current EU Cosmetic Products Regulation (1223/2009) on labeling of products containing ENPs (EC, 2009). The observed measurement uncertainties based on the precision of 3.9–8.8% allow the correct identification of TiO<sub>2</sub> ENPs in the sunscreen as a prerequisite for the successful application of EU Cosmetic Products Regulation. This study confirms that the trueness of the PSD determined by AF4-MALS-ICP-MS analysis has to be taken into account carefully as there is no sunscreen reference material with a certified TiO<sub>2</sub> ENPs size value available. The same issue has been previously emphasized by Linsinger et al. (Velimirovic et al., 2020) and Loeschner et al. (Loeschner et al., 2015) for ENPs in food. In earlier studies, limited robustness towards changes in the experimental protocol, often considered as minor by the operator, have been identified as a major factor introducing uncertainty in the analytical data. Such changes may also lead to low reproducibility of the analytical data. Therefore, it is of the utmost importance to provide clear and versatile sample preparation protocols and perform comprehensive inter-laboratory comparison studies. The analysis of cosmetic products with unknown ingredients is still a challenge and would require additional analysis effort.

With regard to the European Commission's recommendation of the definition of nanomaterials (EU 2011/696) (EU Commission, 2011) (EC, 2011) that classifies materials as nanomaterials based on the number-based PSD, the mass-based PSD derived from AF4-ICP-MS analysis has to be used for screening purposes only. In order to meet future EU legislation requirements and use the AF4-ICP-MS method as a confirmatory, the mass-based PSD has to be converted into a number-based PSD, which will be the objective of our future study.

## CRedit authorship contribution statement

**Milica Velimirovic:** Conceptualization, Validation, Formal analysis, Investigation, Writing - original draft, Project administration. **Stephan Wagner:** Conceptualization, Validation, Investigation, Writing - review & editing, Project administration. **Robert Koeber:** Methodology, Validation, Writing - review & editing. **Thilo Hofmann:** Resources, Writing - review & editing, Funding acquisition. **Frank von der Kammer:** Conceptualization, Methodology, Resources, Writing - review & editing, Funding acquisition.

## Acknowledgments

This research has received funding from the European Union's Seventh Programme for research, technological development and demonstration under grant agreement No 604347-2. The authors thank Dr. Vikram Kestens (JRC, IRMM) for his guidance on the intra-laboratory validation plan. Anonymous reviewers are thanked for critically reading the manuscript and suggesting substantial improvements.

## Declaration of competing interests

The authors declare that they have no known competing financial interests or personal relationships that could have appeared to influence the work reported in this paper.

## References

- Babick, F., Mielke, J., Wohlleben, W., Weigel, S., Hodoroaba, V.-D., 2016. How reliably can a material be classified as a nanomaterial? Available particle-sizing techniques at work. *J. Nanopart. Res.* 18, 1–40. <https://doi.org/10.1007/s11051-016-3461-7>.
- Bocca, B., Caimi, S., Senofonte, O., Alimonti, A., Petrucci, F., 2018. ICP-MS based methods to characterize nanoparticles of TiO<sub>2</sub> and ZnO in sunscreens with focus on regulatory and safety issues. *Sci. Total Environ.* 630, 922–930. <https://doi.org/10.1016/j.scitotenv.2018.02.166>.
- Contado, C., Pagnoni, A., 2008. TiO<sub>2</sub> in commercial sunscreen lotion: flow field-flow fractionation and ICP-AES together for size analysis. *Anal. Chem.* 80, 7594–7608. <https://doi.org/10.1021/ac8012626>.
- de la Calle, I., Menta, M., Klein, M., Maxit, B., Séby, F., 2018. Towards routine analysis of TiO<sub>2</sub> (nano-)particle size in consumer products: evaluation of potential techniques. *Spectrochim. Acta B* 147, 28–42. <https://doi.org/10.1016/j.sab.2018.05.012>.
- EC, 2002. COMMISSION DECISION 2002/657/EC of 12 August 2002 Implementing Council Directive 96/23/EC Concerning the Performance of Analytical Methods and the Interpretation of Results.
- Cosmetic Products Regulation 1223/2009, The European Parliament and of the Council. EC.
- EC, 2011. Commission recommendation of 18 October 2011 on the definition of nano-material (text with EEA relevance) (2011/696/EU). *Off. J. Eur. Union* 275, 38–40.
- EC, 2016. Notes of Guidance for Testing of Cosmetic Ingredients and their Safety Evaluation by the SCC, SCCS/1564/15.
- Gao, X., Lowry, G.V., 2018. Progress towards standardized and validated characterizations for measuring physicochemical properties of manufactured nanomaterials relevant to nano health and safety risks. *NanoImpact* 9, 14–30. <https://doi.org/10.1016/j.impact.2017.09.002>.
- Holcombe, D. (Ed.), 1998. *The Fitness for Purpose of Analytical Methods - A Laboratory Guide to Method Validation and Related Topics*. LGC, Teddington (UK) (ISBN 0-948926-12-0).
- Kammer, F. von der, Legros, S., Hofmann, T., Larsen, E.H., Loeschner, K., 2011. Separation and characterization of nanoparticles in complex food and environmental samples by field-flow fractionation. *TrAC - Trends Anal. Chem.* 30, 425–436. <https://doi.org/10.1016/j.trac.2010.11.012>.
- Kammer, F. von der, Ferguson, P.L., Holden, P.A., Masion, A., Rogers, K.R., Klaine, S.J., Koelmans, A.A., Horne, N., Unrine, J.M., 2012. Analysis of engineered nanomaterials in complex matrices (environment and biota): general considerations and conceptual case studies. *Environ. Toxicol. Chem.* 31, 32–49. <https://doi.org/10.1002/etc.723>.
- Linsinger, T.P.J., Chaudhry, Q., Delahu, V., Delahaut, P., Dudkiewicz, A., Grombe, R., Kammer, F. von der, Larsen, E.H., Legros, S., Loeschner, K., Peters, R., Ramsch, R., Roebben, G., Tiede, K., Weigel, S., 2013. Validation of methods for the detection and quantification of engineered nanoparticles in food. *Food Chem.* 138, 1959–1966. <https://doi.org/10.1016/j.foodchem.2012.11.074>.
- Loeschner, K., Navratilova, J., Grombe, R., Linsinger, T.P.J., Købler, C., Mølhave, K., Larsen, E.H., 2015. In-house validation of a method for determination of silver nanoparticles in chicken meat based on asymmetric flow field-flow fractionation and inductively coupled plasma mass spectrometric detection. *Food Chem.* 181, 78–84. <https://doi.org/10.1016/j.foodchem.2015.02.033>.
- López-Heras, I., Madrid, Y., Cámara, C., 2014. Prospects and difficulties in TiO<sub>2</sub> nanoparticles analysis in cosmetic and food products using asymmetrical flow field-flow fractionation hyphenated to inductively coupled plasma mass spectrometry. *Talanta* 124, 71–78. <https://doi.org/10.1016/j.talanta.2014.02.029>.
- Magnusson, B., Örnemark, U., 2014. *Eurachem Guide: The Fitness for Purpose of Analytical Methods – A Laboratory Guide to Method Validation and Related Topics*, 2nd ed. ISBN 978-91-87461-59-0. Available from. <http://www.eurachem.org>.
- Müller, D., Cattaneo, S., Meier, F., Welz, R., de Vries, T., Portugal-Cohen, M., Antonio, D.C., Cascio, C., Calzolari, L., Gilliland, D., de Mello, A., 2016. Inverse supercritical fluid extraction as a sample preparation method for the analysis of the nanoparticle content in sunscreen agents. *J. Chromatogr. A* 1440, 31–36. <https://doi.org/10.1016/j.chroma.2016.02.060>.
- Neubauer, E., Kammer, F.D. von der, Hofmann, T., 2013. Using FLOWFFF and HPSEC to determine trace metal–colloid associations in wetland runoff. *Water Res.* 47, 2757–2769. <https://doi.org/10.1016/j.watres.2013.02.030>.
- Nischwitz, V., Goenaga-Infante, H., 2012. Improved sample preparation and quality control for the characterisation of titanium dioxide nanoparticles in sunscreens using flow field flow fractionation on-line with inductively coupled plasma mass spectrometry. *J. Anal. At. Spectrom.* 27, 1084. <https://doi.org/10.1039/c2ja10387g>.
- Philippe, A., Košík, J., Welle, A., Guigner, J.-M., Clemens, O., Schaumann, G.E., 2018. Extraction and characterization methods for titanium dioxide nanoparticles from commercialized sunscreens. *Environ. Sci. Nano.* 5, 191–202. <https://doi.org/10.1039/C7EN00677B>.
- Thompson, M., Ellison, S.L.R., Wood, R., 2002. *Harmonized guidelines for single laboratory validation of methods of analysis (IUPAC Technical Report)*. *Pure Appl. Chem.* 74, 835–855.
- Velimirovic, M., Wagner, S., Monikh, F.A., Uusimäki, T., Kaegi, R., Hofmann, T., Kammer, F. von der, 2020. Accurate quantification of TiO<sub>2</sub> nanoparticles in commercial sunscreens using standard materials and orthogonal particle sizing methods for verification. *Talanta* 215, 120921. <https://doi.org/10.1016/j.talanta.2020.120921>.
- Wagner, S., Legros, S., Loeschner, K., Liu, J., Navratilova, J., Grombe, R., Linsinger, T.P.J., Larsen, E.H., Kammer, F. von der, Hofmann, T., 2015. First steps towards a generic sample preparation scheme for inorganic engineered nanoparticles in a complex matrix for detection, characterization, and quantification by asymmetric flow-field flow fractionation coupled to multi-angle light scattering and ICP-MS. *J. Anal. At. Spectrom.* 30, 1286–1296. <https://doi.org/10.1039/C4JA00471J>.